Journal of Materials Science & Technology 34 (2018) 2183–2188

Contents lists available at ScienceDirect

Journal of Materials Science & Technology

journal homepage: www.jmst.org

Achieving ultra-high strength friction stir welded joints of high nitrogen stainless steel by forced water cooling

H. Zhang [a,b], D. Wang [a,*], P. Xue [a], L.H. Wu [a], D.R. Ni [a], B.L. Xiao [a], Z.Y. Ma [a,b,**]

[a] Shenyang National Laboratory for Materials Science, Institute of Metal Research, Chinese Academy of Sciences, 72 Wenhua Road, Shenyang 110016, China
[b] University of Chinese Academy of Sciences, 19 Yuquan Road, Beijing 100049, China

ARTICLE INFO

Article history:
Received 1 December 2017
Received in revised form 22 February 2018
Accepted 19 March 2018
Available online 3 April 2018

Keywords:
Friction stir welding
Stainless steels
Mechanical properties
Corrosion

ABSTRACT

The microstructure and properties of water-cooled and air-cooled friction stir welded (FSW) ultra-high strength high nitrogen stainless steel joints were comparatively studied. With additional rapid cooling by flowing water, the peak temperature and duration at elevated temperature during FSW were significantly reduced. Compared to those in the air-cooled joint, nugget zone with finer grains (900 nm) and heat affected zone with higher dislocation density were successfully obtained in the water-cooled joint, leading to significantly improved mechanical properties. The wear of the welding tool was significantly reduced with water cooling, resulting in better corrosion resistance during the immersion corrosion test.

1. Introduction

Low nickel and nickel-free high nitrogen stainless steels (HNSs) have recently been developed, aimed at reducing the amount of expensive alloy elements and improving the mechanical properties and localized corrosion resistance. Nitrogen, as a powerful austenite stabilizer, has many beneficial effects on the properties of high alloyed steels [1,2], therefore, HNSs exhibit great promise in many industrial fields.

The welding of HNSs has always been a serious challenge. During traditional fusion welding, nitrogen loss was often detected in the weld pool [3]. The desorption of nitrogen could induce a large number of pores, and formed Cr nitrides in the heat affected zone (HAZ) also reduced the properties of the joints. Furthermore, large heat-input of fusion welding was not beneficial to the mechanical properties of the joints. The lack of reliable joining methods has hindered the development and application of HNSs.

Friction stir welding (FSW) as a solid-state joining method is initially applied primarily to the welding of aluminum and magnesium alloys [4–7]. It has shown great advantages in the welding of high strength steels due to its relatively low heat-input [8–11]. FSW is also considered as an effective method of avoiding nitrogen loss and precipitation of Cr nitrides during the welding of HNSs [12].

Cold-rolled HNSs have high strength up to about 1.4 GPa with relatively good elongation, and after 70% cold-rolling strain, an ultra-high strength of 2.2 GPa could be achieved [13,14]. Due to the high nitrogen content, no martensitic transformation occurred during cold rolling. This nonmagnetic austenitic single phase steel with the combination of superior mechanical properties and corrosion resistance could meet the harsh requirements of various fields, such as the chemical industry, the oil industry and the military.

So far, solid-solution state HNSs have mainly been selected for FSW [15,16]. Miyano et al. [17] optimized the welding parameters of HNS, and high strength was achieved in the nugget zone (NZ). Post-weld heat treatment of FSW HNS joint was performed by Du et al. [18], uniform microstructure after heat treatment led to increased elongation. Wang et al. [12] reported that 100% joint efficiency of FSW HNS joint could be achieved via carefully controlling the heat-input of FSW. However, the ultra-high strength of cold-rolled HNSs made the FSW even harder, and to our best knowledge, there are no reports on the welding of cold-rolled HNSs.

There are two major problems in FSW of high strength steels, i.e., the service life of the welding tools and the softening in the HAZ. Polycrystalline cubic boron nitride (pcBN), tungsten based alloys, and tungsten carbide were commonly selected as the candidate materials for FSW of steels. However, brittle fracture and boride formation induced tool wear were reported when pcBN tools was applied [19,20]. The ultra-high strength of cold-rolled HNSs would cause the fracture of pcBN tools more frequently.

* Corresponding author.
** Corresponding author at: Shenyang National Laboratory for Materials Science, Institute of Metal Research, Chinese Academy of Sciences, 72 Wenhua Road, Shenyang, 110016, China.
E-mail addresses: dongwang@imr.ac.cn (D. Wang), zyma@imr.ac.cn (Z.Y. Ma).

https://doi.org/10.1016/j.jmst.2018.03.014
1005-0302/

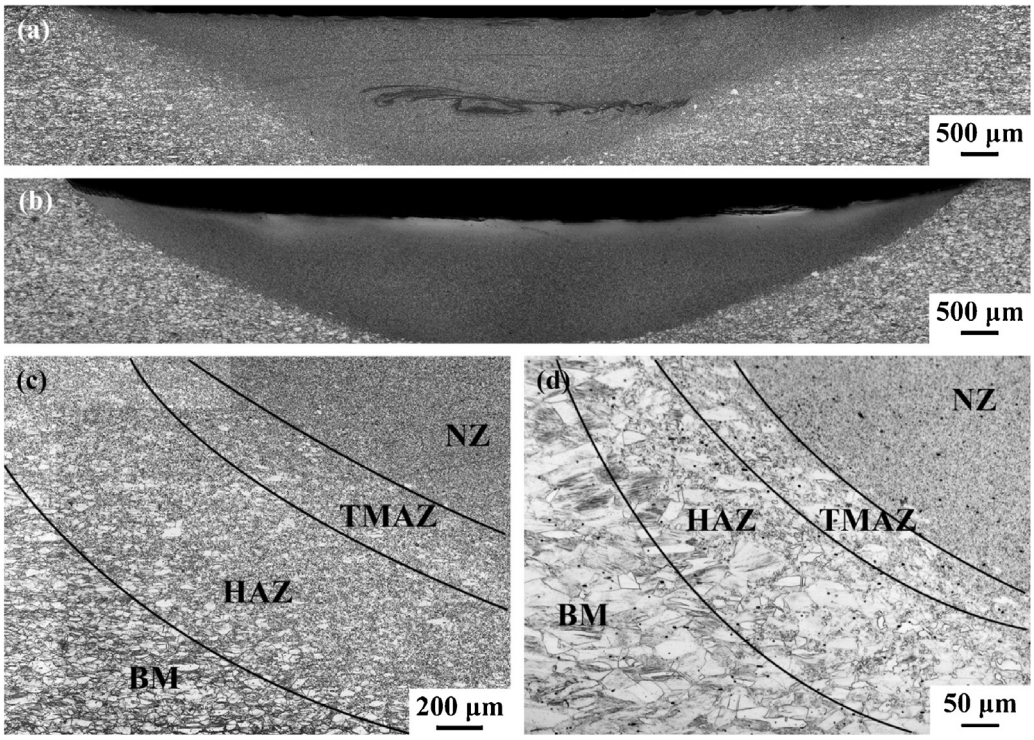

Fig. 1. Cross-sectional macrographs of (a) air-cooled and (b) water-cooled FSW HNS joints; detailed microstructures of (c) air-cooled and (d) water-cooled joints.

W-Re alloys showed better toughness compared to pcBN. However, the tool wear during welding was still the major problem. Sato et al. [21] investigated the tool wear and reactions in a FSW 304 stainless steel joint, and found that the wear debris had harmful effect on the properties of the joints. Furthermore, the cost of FSW tools for steel was very high, thus reducing tool wear during welding is of great significance.

For the ultra-high strength steels strengthened by high density of dislocations, thermal cycle of welding would significantly reduce the dislocation density in the HAZ, with the HAZ being the weakest zone of the joints. Furthermore, Park et al. [15] reported that Cr-rich particles would also precipitate in the HAZ of FSW HNS joints, deteriorating the corrosion resistance. To improve the properties of the joints, the softening of the HAZ should be alleviated. Thus, low heat-input joining methods are highly desirable. Among them, submerged FSW has already been proven to be a feasible method of achieving high-property joints in Cu, Al alloys and steels [7,22–24]. Furthermore, with reduced temperature during welding, enhanced difference in hardness between welding tool and workpiece could be possibly achieved, thus the wear of tool might be alleviated.

In this study, we report, to the best of our knowledge, the subjection of a cold-rolled HNS to submerged FSW with rapid water cooling for the first time. The aim is to provide an effective method for the FSW of high strength steels with improved joint properties and reduced tool wear.

2. Experimental procedure

2 mm thick cold-rolled HNS sheets 140 mm in length and 120 mm in width were used in this study. The chemical composition was Fe–18.4Cr–15.8Mn–2.2Mo–0.66N–0.04C. A W-25Re alloy welding tool with an 11-mm-dia shoulder and 5.7-mm-dia cylindrical pin 1.7 mm in length was adopted. Air cooling and water cooling were applied during different welding processes, respectively. An argon gas shield was employed during FSW in air to prevent the oxidation of the joint, and flowing water was used to cool down the joint during water-cooling FSW. For water-cooled FSW, the water was drained though a pipe rapidly in order to achieving a high cooling rate and constant temperature of the joint.

The heat-input of submerged FSW should be perfectly balanced. If the heat-input is too low, the material flow would be insufficient, resulting in the formation of welding defects or even causing damage to the welding tool. For example, when the rotating rate was reduced to be below 500 rpm, obvious damage to the welding tool was observed. However, if the heat-input is too high, the cooling effect of water will be less effective, resulting in decreased mechanical properties of the joints and severer tool wear due to softening of the welding tool. In this study, a tool rotating rate of 500 rpm and a welding speed of 100 mm/min (abbreviated as 500–100) were determined to be the lowest match of heat input to achieve defect-free joint after experiments.

The cross-section of the joints perpendicular to the welding direction was observed by optical microscopy (OM). The polished specimens were electrolytically etched in a 10% oxalic acid solution. Electron probe micro-analyzer (EPMA) was used to examine the element distribution for identifying the wear of the welding tool. Electron backscattered diffraction (EBSD) was used to analyze the grain size. The specimens for EBSD analysis were prepared by electrolytic polishing with a 10% perchloric acid, and 90% ethanol solution at 30 V. The microstructure features were characterized by transmission electron microscopy (TEM).

The tensile specimens were cut perpendicular to the welding direction with a gauge length of 40 mm, a width of 5 mm, and thickness of 1.7 mm. Tensile tests were carried out at a strain rate of $1 \times 10^{-3}\ s^{-1}$ using a Shimadzu AG-100kNG test machine. Vickers hardness tests were performed on the cross-section along the mid-thickness of the FSW joints using a 200 g load for 15 s. Temperature profiles during FSW were measured using K-type thermocouples that were embedded in the bottom layer of the workpiece close to the tool pin.

Intergranular immersion corrosion tests were performed to detect the susceptibility of the FSW joints following Practice B in

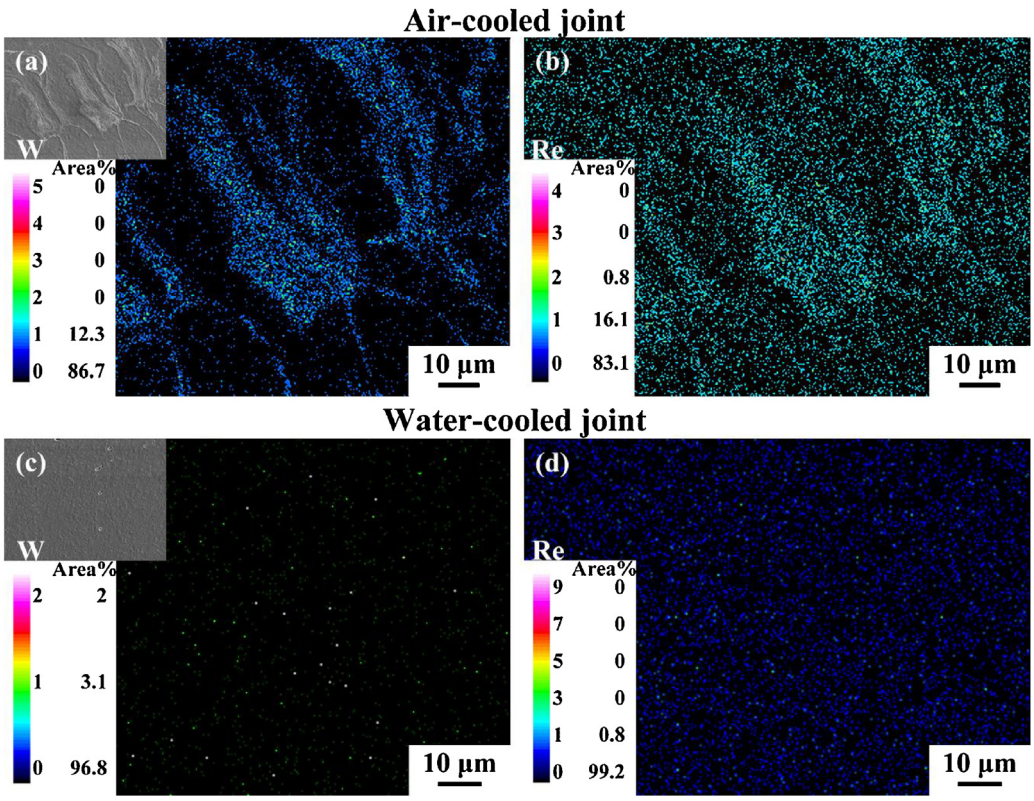

Fig. 2. W and Re distribution mapping of (a, b) air-cooled and (c, d) water-cooled FSW HNS joints.

ASTM A262 standard. The specimens were immersed in a boiling ferric sulfate-sulfuric acid solution for 30 min at a constant temperature of 130 °C. 3D surface microscopy Keyence VHX-1000 was used to represent the corroded surface and the depth of corrosion.

3. Results

3.1. Microstructural characterization

The cross-sectional macrographs of air-cooled and water-cooled FSW HNS joints are shown in Fig. 1(a) and (b). Basin-like NZs were observed under both FSW conditions. In the middle layer of the NZ of the air-cooled joint, a heavily corroded band with a wavy shape could be clearly observed in Fig. 1(a).

In our previous study, such a corroded band in FSW joints of solid solution state HNS was confirmed to result from tool wear and could not be avoided though different welding parameters were tried [25]. Similar phenomena were also reported by Steuwer et al. [26] in FSW HSLA-65 steel joints. It is important to note that in the water-cooled FSW joint (Fig. 1(b)), no such heavily corroded bands could be detected.

The detailed microstructure of the joints is shown in Fig. 1(c) and (d). Deformation bands could be clearly observed in the BM, indicating highly deformed microstructure after cold rolling. The thermos-mechanically affected zone (TMAZ) exhibited partially recrystallized microstructure characterized by fine recrystallized grains and deformed coarse grains with vague grain boundaries. Due to the high storage energy in the BM and relatively high temperature during welding, the HAZs of both joints also exhibited a partial recrystallization characteristic, consisting of coarse grains retained from the less deformed grains in the BM and fine recrystallized grains resulting from highly deformed grains (Fig. 1(c) and (d)). The air-cooled joint had a HAZ width of 1.6 mm (Fig. 1(c)), whereas the width of the water-cooled HAZ was significantly reduced to about 0.4 mm (Fig. 1(d)) due to rapid cooling of flowing water.

Tungsten and rhenium distribution mapping results for the air-cooled and water-cooled joints are given in Fig. 2. The mapping locations were selected at the middle layer of the NZ on the advancing side, where the tool wear bands were mainly observed. The content of elements was presented by the color of the points in the map and the 0 Area% in the bottom left inserts indicated the occupied area of the BM. Concentration of W and Re could be clearly observed in the air-cooled joint (Fig. 2(a) and (b)). The distribution of W and Re corresponded to the wavy-shape band shown in Fig. 1(a). Since there were no W and Re elements in the BM, the tool wear in the air-cooled joint could be confirmed. By comparison, in the water-cooled joint, almost no W and Re were detected, the 0 Area% of W and Re was 96.8% and 99.2%, respectively, indicating that the wear of welding tool was significantly reduced for water-cooled FSW (Fig. 2(c) and (d)).

3.2. Mechanical properties

The hardness profiles of the FSW joints are shown in Fig. 3. Both joints show the W-type hardness profile with the HAZs being identified as the lowest hardness regions. Compared to the air-cooled joint, the water-cooled joint exhibited an increase in the lowest hardness value in the HAZ, and the highest hardness of the NZ was close to that of the BM.

Table 1 shows the mechanical properties of the FSW joints. The water cooling increased the joint strength significantly. Higher strength up to about 1.3 GPa was obtained via additional cooling, which was close to that of the BM (1.6 GPa). The failure occurred at the HAZs for both joints, which was consistent with the hardness distribution profiles. The elongation of FSW joints slightly increased compared to that of the ultra-high strength BM.

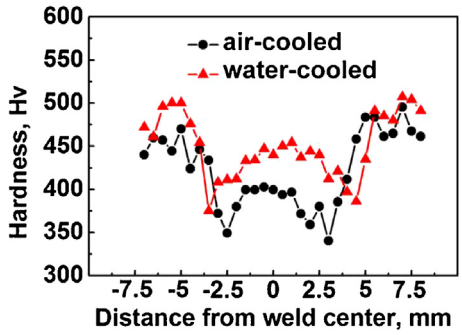

Fig. 3. Hardness profiles in cross-sections of FSW HNS joints.

Table 1
Mechanical properties of FSW HNS joints obtained via different cooling methods.

Sample	Yield strength (MPa)	Tensile strength (MPa)	Elongation (%)	Joint efficiency
BM	1350 ± 40	1613 ± 74	7	–
Air-cooled joint	944 ± 35	1150 ± 23	13.3	71.3%
Water-cooled joint	1071 ± 27	1295 ± 32	11	80.3%

3.3. Corrosion behavior

As can be observed in Fig. 4, the tool wear band in the air-cooled joint was sensitive to corrosion. After a 30 min immersion corrosion test, the tool wear band developed into a ditch-like structure with a depth of about 70 μm. On the other hand, in the water-cooled joint with obviously reduced tool wear, the corrosion resistance of the NZ was significantly improved. The NZ was uniformly corroded with a depth of about 29 μm.

4. Discussion

The microstructural differences between two joints would greatly affect the mechanical properties and corrosion behavior. As a kind of dislocation strengthened ultra-high strength steel, high densities of dislocations and stacking faults could be observed in the BM (Fig. 5(a)). However, due to the thermal cycle of FSW, the dislocation densities of the HAZs in both joints were significantly reduced (Fig. 5(b) and (c)), leading to decreased hardness and strength.

Both HAZs exhibited the characteristics of recrystallization microstructure, as shown in Fig. 5(b) and (c). In the HAZ of the air-cooled joint (Fig. 5(b)), low dislocation density and coarse annealing twins could be observed, which indicated that the recrystallization was sufficient. On the other hand, very fine grains with relatively high density of dislocations were the main characteristic of the HAZ in the water-cooled joint (Fig. 5(c)), indicative of less sufficient recrystallization compared to that in the air-cooled joint. Therefore, significant increase in the lowest hardness and joining strength was achieved in the water-cooled joint.

The NZs of the two joints also exhibited a significant difference. The grains in the NZ for the water-cooled joint were significantly

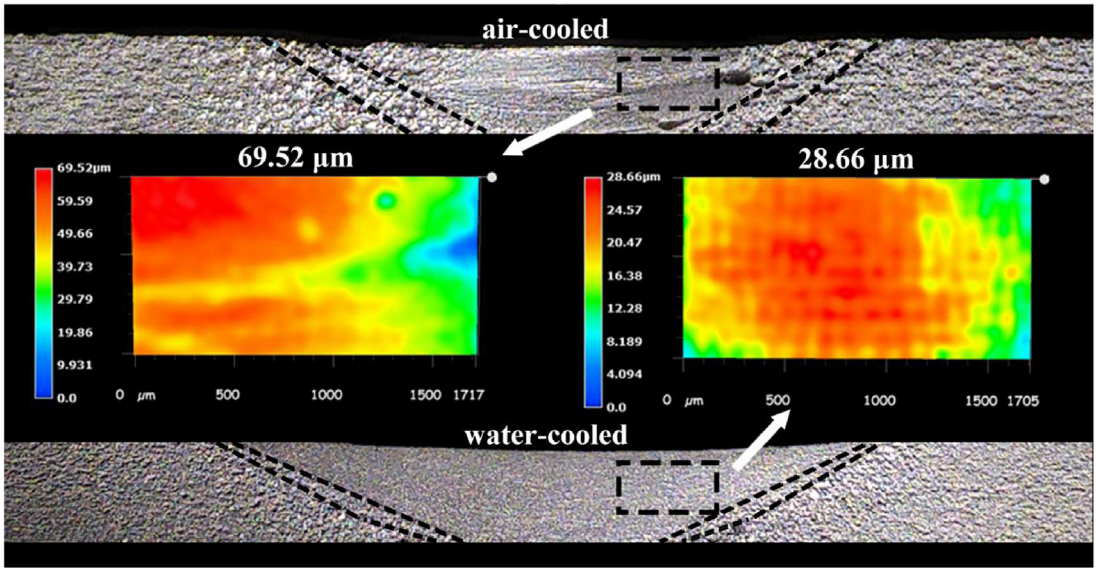

Fig. 4. Cross-sectional macrographs and 3D surface morphologies of FSW joints after immersion corrosion test.

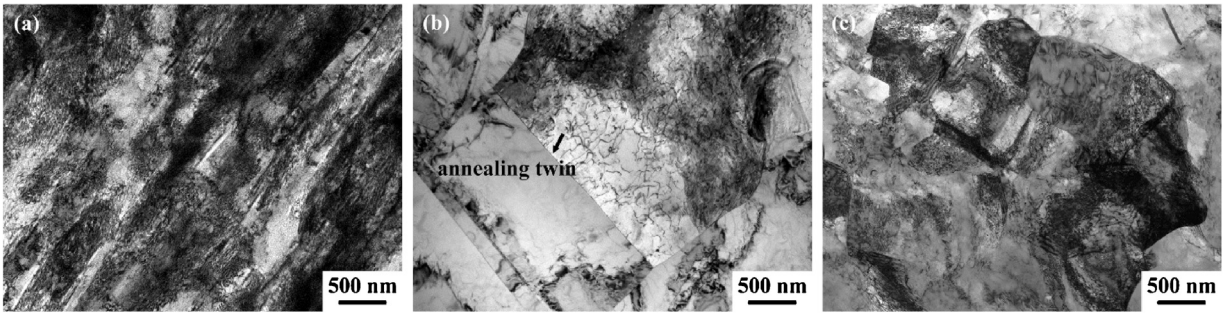

Fig. 5. Microstructure of (a) cold-rolled HNS, (b) HAZ of air-cooled joint, (c) HAZ of water-cooled joint.

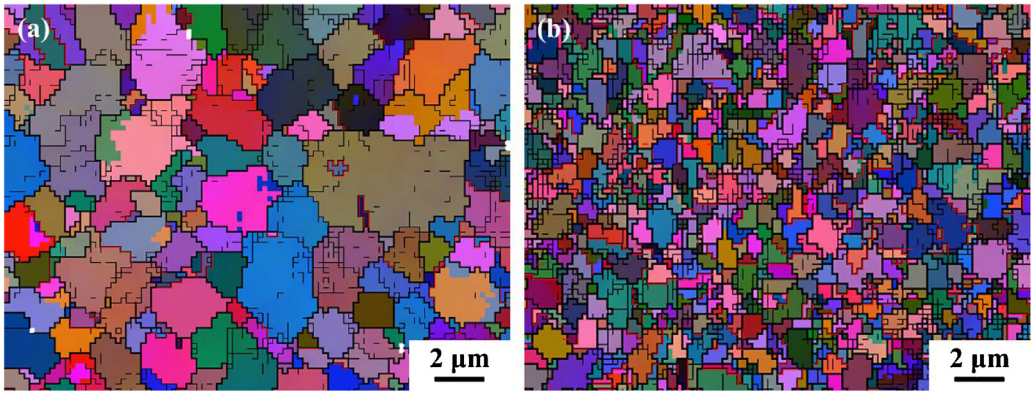

Fig. 6. EBSD maps of NZs of (a) air-cooled and (b) water-cooled joints.

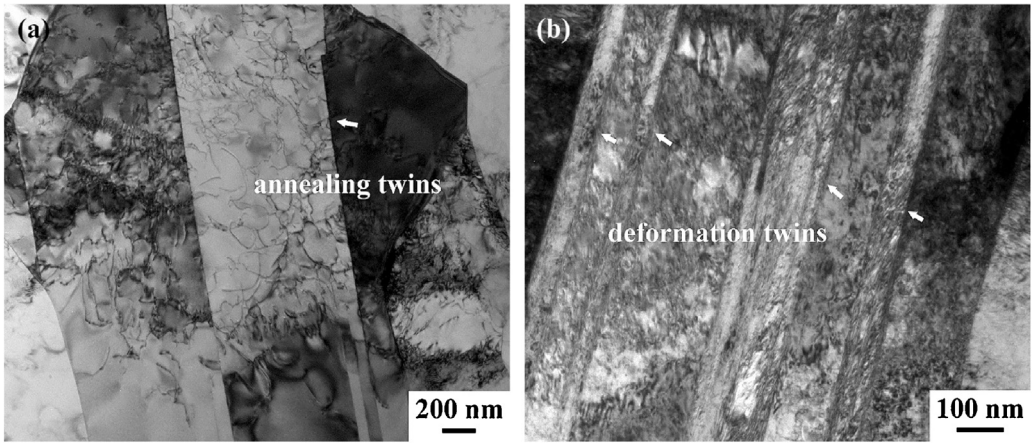

Fig. 7. Microstructure of NZs of (a) air-cooled and (b) water-cooled joints.

refined to about 900 nm (Fig. 6(b)), while those for the air-cooled joint were 2 μm (Fig. 6(a)). On the other hand, high density of dislocations and deformation twins were observed in the NZ of the water-cooled joint (Fig. 7(b)), while relatively low dislocation density and coarse annealing twins were detected in the NZ of the air-cooled joint (Fig. 7(a)). The improvement of the highest hardness of the NZ in the water-cooled joint was mainly attributed to the ultra-fine grain microstructure and high defect density.

The main differences between the air-cooled joint and water-cooled joint were peak temperature and high temperature exposure duration. The temperature curves during FSW of the bottom layer close to the welding tool pin are shown in Fig. 8. The peak temperature near the tool pin in the water-cooled joint was about 540 °C, which was significantly lower than that in the air-cooled one (800 °C). The duration at high temperature range was also cut by half via forced cooling by flowing water. It can be deduced that the temperature differences in the NZs of both joints would be even larger. All of these factors had beneficial impact on maintaining the ultra-fine grain microstructure in the NZ and reducing the dislocation consumption in the HAZ for the water-cooled joint. As a result, high strength and hardness were achieved in the water-cooled joint.

The reduction of the tool wear could also be explained by temperature curves. It has been reported that the yield strength of HNSs at high temperature range showed little change [27]. However, the yield strength of W-25Re alloy drops sharply at elevated temperature, the tensile strength of W-26 Re alloy was about 690 MPa

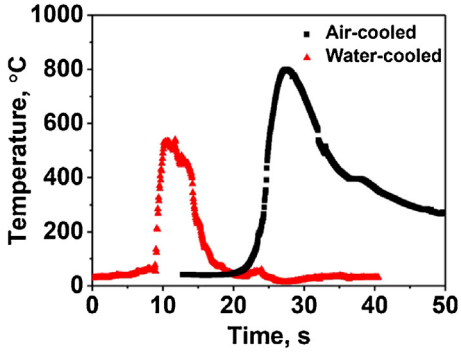

Fig. 8. Temperature histories during FSW of the bottom layer of workpiece close to welding tool pin.

at 1000 °C, only about half of the strength at room temperature [28]. It can be deduced that the tool wear in the air-cooled joint was mainly attributed to insufficient strength and hardness of W-Re alloy at high temperatures. With highly efficient water cooling, the hardness of the welding tool would be mostly retained during FSW. According to the study of Savitskii [29], if the peak temperature decreased from 1000 °C to 800 °C, the hardness of W-25Re alloy would increase from about 130 kg/mm^2 to 200 kg/mm^2. As a result, the tool wear in the water-cooled joint was significantly reduced due to the retaining of relatively high hardness of W-25Re tool at relatively low process temperature.

5. Conclusions

The feasibility of friction stir welding (FSW) for joining ultra-high strength cold-rolled high nitrogen stainless steel (HNS) was explored. Different cooling methods were used to control the microstructures and optimize the overall properties. The conclusions can be summarized as follows:

(1) Defect-free joints of ultra-high strength HNS could be successfully achieved via FSW in air and under water. Nugget zone (NZ) with uniform fine grains and heat affected zones (HAZs) with partial recrystallization characteristic were obtained in these two joints.
(2) The peak temperature and high temperature duration during FSW were significantly reduced via quick flowing water cooling. As a result, optimized microstructure of the NZ with ultra-fine grains and the HAZs with high density of dislocations was successfully obtained in the water-cooled joint. The welding tool wear was reduced simultaneously.
(3) Compared to the air-cooled joint, the water cooled joint exhibited significantly improved mechanical properties with a joint strength of 1.3 GPa. Furthermore, the corrosion resistance of the NZ was also substantially improved in the water-cooled joint due to significantly reduced tool wear.

Acknowledgment

This work was supported by the National Natural Science Foundation of China under grant Nos. 51201163, 51331008 and 51671190.

References

[1] J.W. Simmons, Mater. Sci. Eng. A 207 (1996) 159–169.
[2] F.M. Bayoumi, W.A. Ghanem, Mater. Lett. 59 (2005) 3311–3314.
[3] I. Woo, Y. Kikuchi, ISIJ Int. 42 (2002) 1334–1343.
[4] R.S. Mishra, Z.Y. Ma, Mater. Sci. Eng. Rep. 50 (2005) 1–78.
[5] R.Z. Xu, D.R. Ni, Q. Yang, C.Z. Liu, Z.Y. Ma, J. Mater. Sci. Technol. 32 (2016) 76–88.
[6] A.H. Feng, D.L. Chen, Z.Y. Ma, W.Y. Ma, R.J. Song, Acta Metall. Sin. (Engl. Lett.) 27 (2014) 723–729.
[7] B.B. Wang, F.F. Chen, F. Liu, W.G. Wang, P. Xue, Z.Y. Ma, J. Mater. Sci. Technol. 33 (2017) 1009–1014.
[8] H. Fujii, R. Ueji, Y. Morisada, H. Tanigawa, Scr. Mater. 70 (2014) 39–42.
[9] Y.S. Sato, H. Yamanoi, H. Kokawa, T. Furuhara, Scr. Mater. 57 (2007) 557–560.
[10] P. Xue, Y. Komizo, R. Ueji, H. Fujii, Mater. Sci. Eng. A 606 (2014) 322–329.
[11] F.C. Liu, Y. Hovanski, M.P. Miles, C.D. Sorensen, T.W. Nelson, J. Mater. Sci. Technol. 34 (2018) 39–57.
[12] D. Wang, D.R. Ni, B.L. Xiao, Z.Y. Ma, W. Wang, K. Yang, Mater. Des. 64 (2014) 355–359.
[13] S.C. Sun, J.W. Mu, Z.H. Jiang, C.T. Ji, J.S. Lian, Q. Jiang, Mater. Sci. Technol. 30 (2013) 146–151.
[14] M. Talha, C.K. Behera, O.P. Sinha, Mater. Sci. Eng. C 47 (2015) 196–203.
[15] S.H.C. Park, Y.S. Sato, H. Kokawa, K. Okamoto, S. Hirano, M. Inagaki, Mater. Sci. Forum 539–543 (2007) 3757–3762.
[16] H.B. Li, Z.H. Jiang, H. Feng, S.C. Zhang, L. Li, P.D. Han, R.D.K. Misra, J.Z. Li, Mater. Des. 84 (2015) 291–299.
[17] Y. Miyano, H. Fujii, Y. Sun, Y. Katada, S. Kuroda, O. Kamiya, Mater. Sci. Eng. A 528 (2011) 2917–2921.
[18] D. Du, R. Fu, Y. Li, L. Jing, Y. Ren, K. Yang, Mater. Sci. Eng. A 616 (2014) 246–251.
[19] R. Rai, A. De, H.K.D.H. Bhadeshia, T. DebRoy, Sci. Technol. Weld. Join. 16 (2011) 325–342.
[20] S.H.C. Park, Y.S. Sato, H. Kokawa, K. Okamoto, S. Hirano, M. Inagaki, Metall. Mater. Trans. A 40 (2009) 625–636.
[21] Y.S. Sato, M. Muraguchi, H. Kokawa, Mater. Sci. Forum 675–677 (2011) 731–734.
[22] P. Xue, B.L. Xiao, Q. Zhang, Z.Y. Ma, Scr. Mater. 64 (2011) 1051–1054.
[23] S. Shashi Kumar, N. Murugan, K.K. Ramachandran, Mater. Sci. Forum 830–831 (2015) 314–318.
[24] P. Xue, H. Zhao, Y. Komizo, Z.Y. Ma, Proceedings of the 1st International Joint Symposium on Joining and Welding (2013) 445–448.
[25] H. Zhang, D. Wang, P. Xue, L.H. Wu, D.R. Ni, Z.Y. Ma, Mater. Des. 110 (2016) 802–810.
[26] A. Steuwer, S.J. Barnes, J. Altenkirch, R. Johnson, P.J. Withers, Metall. Mater. Trans. A 43 (2011) 2356–2365.
[27] J. Ganesh Kumar, M. Chowdary, V. Ganesan, R.K. Paretkar, K. Bhanu Sankara Rao, M.D. Mathew, Nucl. Eng. Des. 240 (2010) 1363–1370.
[28] F.F. Schmidt, H.R. Ogden, DTIC Document, 1963.
[29] E.M. Savitskii, M.A. Tylkina, S.I. Ipatova, E.I. Pavlova, Met. Sci. Heat Treat. 2 (1960) 483–486.